Int. J. Heat Mass Transfer. Vol. 36, No. 6, pp. 1425–1434, 1993
Printed in Great Britain

0017–9310/93 $6.00 + 0.00

Experimental determination of the volumetric heat transfer coefficient between stream of air and ceramic foam

L. B. YOUNIS and R. VISKANTA
Heat Transfer Laboratory, School of Mechanical Engineering, Purdue University, West Lafayette, IN 47909, U.S.A.

(*Received* 24 *February* 1992 *and in final form* 11 *August* 1992)

Abstract—An experimental investigation is described that characterizes heat transfer between a heated air stream and ceramic foam. An apparatus is designed to determine the volumetric heat transfer coefficient between the foam and a stream of air using a single-blow transient technique. Experiments are reported on different mean pore diameter specimens. The governing conservation equations of energy for both the gas and the solid phases with appropriate boundary and initial conditions are solved using a finite-difference procedure. A nonlinear, least-square fit of predicted and measured gas temperatures is used to determine the volumetric heat transfer coefficient between air and ceramic foams. Two different types of ceramic foams are investigated, and the results obtained are compared. Heat transfer coefficient correlations are developed for each different mean pore diameter of ceramic foam and for the range of Reynolds numbers between 12 and 563 covered in the experiments.

1. INTRODUCTION

AN IMPORTANT application of porous ceramics is in advanced burners, convection–radiation-converters, low thermal mass structural components for advanced furnaces and combustor-incinerators [1, 2]. Ceramic foams can also be used as catalysts, molten metal filters, heat resistant filters, chemical resistance filters, fillers of contact reaction towers, diffusers, and fluid mixers. For example, in a novel concept of a self-regenerating, combustor-incinerator two porous plates are placed opposite to each other [3]. The combustion air enters through the inlet porous plate. It mixes with the fuel and burns in the chamber, and the combustion products leave through the exit porous plate. A recent survey of industrial combustion systems has identified a large number of applications where porous ceramics (reticulated ceramics, fibrous ceramics, ceramic foams) are being used [1]. Porous materials also find application in porous heat exchangers in which heat exchange is realized between a permeable matrix and a fluid flowing inside it [4].

The physical and chemical properties of reticulated ceramics which make them particularly well-suited for heat recovery applications include a very high surface area per unit volume, low pressure drop, excellent thermal shock characteristics, high temperature durability, and a diverse selection of physical properties which can be engineered through the appropriate selection of material composition and processing parameters. Porous media can be in the form of packed beds, sintered materials or ceramic foams. Ceramic foams have a high porosity (>83%) and high permeability. The ceramic foam passages are much more complex than those of packed beds or sintered metals due to the random shape of pore shape and size.

Development and optimization design of advanced combustion systems which meet pollutant emission standards and/or maintain or increase productivity will require mathematical modeling of the systems. The reduction in time between a system concept and commercialization and the increase in the cost of testing will demand a greater reliance on mathematical models to simulate the systems and reduce the cost and time to develop a product. For mathematical modeling efforts to be successful, it is necessary to have convective heat transfer coefficient data between a gas stream and solid matrix. This is because conduction, convection and radiation heat transfer and chemical heat release due to combustion are intimately coupled, and partitioning of heat transfer between convection and radiation is critically important. Heat conduction in the solid matrix is not that important because the effective thermal conductivity of the solid is relatively low, particularly for reticulated ceramics which have a high porosity (e.g. ~83 to 95%).

Convective heat transfer coefficients for gases flowing through packed beds have been measured and the studies have been reviewed in the literature [5–10]. Even though experiments have been carried out since 1929 [11] to measure the heat transfer coefficients of packed beds, until now no universal correlations have been developed. A valuable study was performed by Furnas [12] and reported by Kitaev *et al.* [13] both on the methodology and on large scale apparatus. Furnas carried out work over the widest range of the different parameters: temperatures up to 1100°C, velocities

NOMENCLATURE

a_v	surface area per unit volume [$m^2\ m^{-3}$]
c_{pg}	specific heat of the gas [$J\ kg^{-1}\ K^{-1}$]
c_s	specific heat of the solid [$J\ kg^{-1}\ K^{-1}$]
d	pore diameter [m]
h	heat transfer coefficient [$W\ m^{-2}\ K^{-1}$]
h_v	volumetric heat transfer coefficient, $a_v h$ [$W\ m^{-3}\ K^{-1}$]
k	thermal conductivity [$W\ m^{-1}\ K^{-1}$]
k^*	thermal conductivity ratio, k_s/k_g
L	thickness of the porous ceramic [m]
Nu	Nusselt number, $h_v d^2/k_g$
Nu_L	Nusselt number at face $x = L$, $h_L L/k_s$
Nu_0	Nusselt number at face $x = 0$, $h_0 L/k_s$
$N_{R\,C}$	radiation to conduction dimensionless parameter, $(\varepsilon\sigma L/k_s)(T_s^3 + T_s T_{sur}^2 + T_s^2 T_{sur} + T_{sur}^3)$
Pr	Prandtl number, $\mu c_{pg}/k_g$
q	heat flux [$W\ m^{-2}$]
Re	Reynolds number, $\rho U d/\mu$
S	minimum function of the least-square fit defined by equation (10)
t	time [s]
T	temperature [K]
U	air velocity [$m\ s^{-1}$]
x	Cartesian coordinate along the specimen length [m]
Z	sensitivity coefficient defined as $\partial T_p^{m+i-1}/\partial h_v^m$.

Greek symbols

Δh_v	volumetric heat transfer coefficient difference [$W\ m^{-3}\ K^{-1}$]
ε	emissivity
ξ	dimensionless coordinate, x/L
θ	dimensionless temperature, $(T - T_{in})/(T_i - T_{in})$
μ	dynamic viscosity [Pa s]
ρ	density [$kg\ m^{-3}$]
σ	Stefan–Boltzmann constant [$W\ m^{-2}\ K^{-4}$]
ϕ	porosity
τ	dimensionless time, $h_v t/\rho_s c_s$.

Subscripts

e	experimental
g	refers to gas
i	denotes inlet
in	refers to initial
L	refers to face at $x = L$
0	refers to face at $x = 0$
p	predicted
s	refers to solid
sur	refers to surrounding.

from 0.6 to 1.8 m s^{-1}, and test samples of the most diverse materials, from 4 to 70 mm in diameter. His work contributed to the understanding of the processes and aided the research of others to follow.

A thorough search of literature has revealed no experimental convective heat transfer coefficient data for high (>83%) porosity foams. There are extensive data and empirical correlations for convective heat transfer for packed beds covering a large range of particle diameters, Reynolds numbers and fluids in the sources which have been identified in the previous paragraph. Eroshenko and Yaskin [5] reviewed the Nusselt number correlations for sintered metals and found that the exponent of the Reynolds number in the empirical Nu vs Re number correlations, ranged from 0.56 to 1.84. There was also disagreement among investigators with respect to the dependence of the Nusselt number on the relative porous layer thickness and on the choice of the characteristic length for defining both the Reynolds and Nusselt numbers. Use of convective heat transfer coefficient correlations obtained with sintered metals to calculate convective heat transfer between a gas stream and ceramic foams yielded unrealistic predictions. This is attributed to several factors such as much lower porosity, mean particle diameter and much higher thermal conductivity for sintered metals than for the foams. For the sake of completeness, heat transfer data reported by Kays and London [14] for cross-rods, screen and sphere matrices should be mentioned. For some of the screen matrices the porosities were quite high ($0.6 < \phi < 0.83$), and the heat transfer coefficient data were correlated in terms of the Colburn j-factor, with the hydraulic diameter being used in the Reynolds number as the characteristic length.

There is a lack of knowledge concerning heat transfer coefficients in porous ceramic foams. A large part of the work done to date was intended for applications to porous sintered metals or packed beds for which the porosity is small ($\phi < 0.4$) and not with high porosity ceramic foams for which $\phi > 0.83$. This paper reports the results from an experimental study aimed at determining volumetric convective heat transfer coefficients between air stream and high porosity ceramic foams. A series of tests have been conducted using the 'single-blow' transient technique to obtain experimental data, and an inverse technique has been used to determine time-averaged convective heat transfer coefficients. The data are analyzed and empirical Nusselt vs Reynolds number correlations are reported.

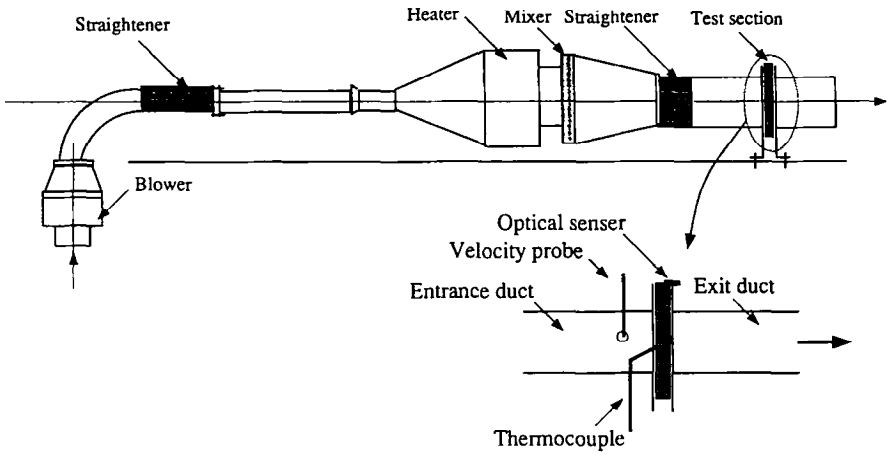

FIG. 1. Schematic diagram of the test apparatus.

2. EXPERIMENTAL APPARATUS AND PROCEDURE

A schematic diagram of the experimental apparatus is shown in Fig. 1. It mainly consists of a low speed wind tunnel, a test section which includes two slide rails to slide a dummy and test specimen, instrumentation, and data acquisition system. There were four thermocouples in front of the dummy specimen, while there were two thermocouples on the front side and two at the back side of the test sample. An optical sensor is placed on the top right side of the test section. The sensor is used to start recording the temperature data and to measure the sliding time.

The test materials are reticulated ceramics (ceramic foams) which are porous materials. Two kinds of test materials were used, namely alumina RETICEL (Al_2O_3, 92% pure) manufactured by Hi-Tech Ceramics, Inc. having different mean pore diameters. The second material tested consisted of cordierite ($2MgO \cdot 2Al_2O_3 \cdot 5SiO_2$) manufactured by Bridgestone Corporation. Table 1 summarizes the specifications of the alumina and cordierite test specimen.

The test is initiated by adjusting powerstats to obtain desired temperature and air velocity, and setting the time needed to reach steady state temperature, which depends on the air velocity for the experiment. With the dummy specimen in position in the test assembly and four thermocouples, at the top, bottom, right and left side of the dummy, the temperature is monitored using the HP-85A computer. A uniform temperature is usually obtained within 1 to 2 h, depending on the air velocity. The experiment begins with turning on the optical sensor by using the HP 6235A triple output power supply and sliding the test specimen in place in the duct. The sliding time varies between 0.13 to 0.58 s. This time is subtracted from the experiment time.

The emf output from the thermocouples was recorded using an HP-85A computer and an HP-3852A data acquisition unit which records and uploads the data. There are 7.3 records per second (or every 0.13 to 0.58 s a data point is recorded). At the end of the experiment the recorded data are printed, and the velocity is measured at the front face of the specimen. The velocity of the air is measured at the end of each experiment. In order to obtain the correct velocity for each specimen with different pore size, the velocity is

Table 1. Physical properties of ceramic foams tested

Average number of pores (cm^{-1})	Average pore diameter (mm)	Bulk density ($g\ cm^{-3}$)	Porosity (%)	Thermal conductivity ($W\ m^{-1}\ K^{-1}$)	Specific heat ($J\ kg^{-1}\ K^{-1}$)
Alumina (92% Al_2O_3, Hi-Tech Ceramics, Inc.)					
4	1.52	0.51	87.0	3.87	824.7
8	0.94	0.61	85.0	3.87	824.7
12	0.76	0.66	83.0	3.82	824.7
18	0.42	0.65	84.0	4.23	824.7
26	0.29	0.66	83.4	2.84	824.7
Cordierite ($2MgO \cdot 2Al_2O_3 \cdot 5SiO_3$, Bridgestone Corporation)					
8	1.25	0.42	85.1	2.60	807.0

measured at the end of the experiment, with the test specimen in place in the duct. The uniform upstream and ambient room temperature used as the initial gas and solid temperature of the matrix, were recorded before each experiment began.

The temperature upstream and downstream of the specimen was measured by a set of thermocouples introduced through the bottom and the top of the Bakelite frame. The foam surface temperature was measured at the two faces of the ceramic foam using contact thermocouples. The thermocouples measuring air temperature in front and behind the faces of the test specimen were corrected for the finite time response. A model was also developed to correct the gas temperature measured by thermocouples for heat conduction and radiation errors [15].

The velocity distribution was measured by a hot wire anemometer (TSI Veloci Calc Model 8350). The velocity probe was inserted into the duct, 1 cm ahead of the test specimen. The air velocity is measured at the end of the experiment by a probe placed in the middle of the duct exactly in front of the front thermocouple. About 50–60 readings are recorded and then averaged during 1–2 s. The velocity profiles across the duct horizontally and vertically were measured for each experiment to ensure the uniformity of the flow.

3. ANALYSIS

3.1. *Physical description of the problem*

A schematic of a one-dimensional specimen of porous material is shown in Fig. 2. A ceramic porous medium of uniform porosity is initially at a uniform temperature and is placed in a stream of a gas which is at a different temperature than the matrix. The gas is at a specific temperature and flows from the left to the right. Because of heat transfer between the gas and the solid matrix, the temperatures of the solid and gas will be changing with time. The fluid flow is steady, and the thermophysical properties of the fluid and solid matrix are assumed to be constant. The velocity of the flow is uniform, i.e. plug flow. In the case of an air–ceramic porous bed, the energy storage in the air is negligible in comparison to the solid since its thermal heat capacity is two orders of magnitude smaller than the thermal capacity of the porous solid.

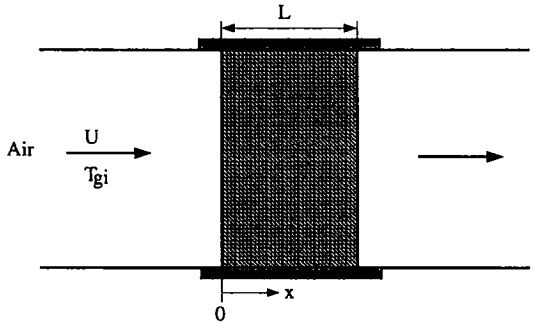

FIG. 2. Schematic diagram of the physical model.

The analysis assumes that the gas is not in thermal equilibrium with the solid matrix. Therefore, separate energy equations are needed to describe energy transfer in these two phases. The resulting conservation equations of energy balances for the fluid and solid are [16–18],

gas:

$$\rho_g c_{pg} U \frac{\partial T_g}{\partial x} = h_v (T_s - T_g) \tag{1}$$

solid:

$$\rho_s c_s \frac{\partial T_s}{\partial t} = \frac{\partial}{\partial x}\left(k_s \frac{\partial T_s}{\partial x}\right) + h_v (T_g - T_s). \tag{2}$$

For the system considered, the boundary conditions for the energy equation of the solid matrix, equation (2), are

$$q = -k_s \frac{\partial T_s}{\partial x} = [h_o (T_{gi} - T_s) - \varepsilon\sigma (T_s^4 - T_{sur}^4)]$$

$$\text{at } x = 0 \tag{3}$$

$$q = -k_s \frac{\partial T_s}{\partial x} = [h_L (T_s - T_{go}) + \varepsilon\sigma (T_s^4 - T_{sur}^4)]$$

$$\text{at } x = L. \tag{4}$$

The inlet condition for the gas temperature, equation (1), is

$$T_g = T_{gi} \quad \text{at } x = 0. \tag{5}$$

The governing equations are non-dimensionalized by introducing dimensionless variables and the gas and solid become, respectively,

$$Re\, Pr \frac{\partial \theta_g}{\partial \xi} = Nu(L/d)(\theta_s - \theta_g) \tag{6}$$

$$Nu \frac{\partial \theta_s}{\partial \tau} = k^*(d/L)^2 \frac{\partial^2 \theta_s}{\partial \xi^2} + Nu(\theta_g - \theta_s). \tag{7}$$

The boundary conditions, equations (3) and (4), in dimensionless form are

$$\frac{\partial \theta_s}{\partial \xi} = Nu_o(\theta_{gi} - \theta_s) - N_{R\text{-}C}(\theta_s - \theta_{sur}) \quad \text{at } \xi = 0 \tag{8}$$

$$\frac{\partial \theta_s}{\partial \xi} = Nu_L(\theta_s - \theta_{go}) + N_{R\text{-}C}(\theta_s - \theta_{sur}) \quad \text{at } \xi = 1. \tag{9}$$

3.2. *Method of solution and validation*

The methodology used to solve equations (6) and (7) and the associated boundary conditions is based on the control volume, finite-difference technique [19]. The unsteady finite-difference form of the energy equation for solid is obtained for each node location by integrating equation (6) over space in the ξ-direction and over time. These algebraic equations are then solved using a line-by-line iterative method. The time dependence is handled by stepping forward in time and retaining a converged solution at each time step.

The numerical scheme has been checked by performing the node number and time increment sensitivity studies. Different numbers of nodes (50, 60, 100, 150 and 200) were used to ensure that the results of these studies were grid independent. The results show that 100 nodes are sufficient to obtain grid independent results. The dimensionless temperature of the gas at $\xi = 1$ for $\tau = 6.94$ differs by 0.0045 for 50 and 100 grids, but the temperature difference for grids of 100 and 150 nodes is 0.001. Hence, 100 nodes are used throughout the calculations [15].

The effect of the time step on the results was also examined. Some selected results for time steps of 0.05, 0.1, 0.2, 0.5 were tested. The values indicate that there is no significant difference between the results using time increments of 0.05 and 0.1. Hence, an increment of 0.05 was chosen for carrying out the calculations [15].

To gain confidence in the numerical methodology for solving the model equations, the computer program was used to predict the temperature distribution in a one-dimensional porous medium. The temperature predictions based on the computer program used in this work are compared with the solution reported by Alifanov *et al.* [8]. Their numerical solution of the boundary-value problem was carried out on the space–time network. The equations were approximated by a monotonic implicit finite-difference scheme of second order accuracy in the space coordinate for a control volume thickness of 0.18 mm and a first order of accuracy in time. The present work used a 0.14 mm control volume thickness. The agreement between the published solution and the temperature of the solid at $x = 0$ predicted in this work for a Nusselt number of 22 is within the accuracy of reading the published graphical results for the temperature distribution.

4. PARAMETER ESTIMATION

The problem under consideration is an inverse one. We seek to find the volumetric heat transfer coefficient between the gas stream and the solid matrix by measuring the time history of the gas and solid temperatures at certain locations.

A parameter estimation technique is used to determine the volumetric heat transfer coefficient between the porous media and a gas. This is accomplished by minimizing the error between predicted (T_p) and measured temperatures (T_e). The summation of the square of the error can be expressed as

$$S = \sum_{i=1}^{r} (T_e^{m+i} - T_p^{m+i})^2 \tag{10}$$

where superscript $m+i$ denotes the time step.

The method is to minimize S at each time step and for each sensor (thermocouple). The sensitivity or the variation of S with a change in the heat transfer coefficient is measured by the differentiation of equation (10) with respect to h_v,

$$\frac{\partial S}{\partial h_v^m} = 2 \sum_{i=1}^{r} (T_e^{m+i-1} - T_p^{m+i-1}) Z^{m+i-1} = 0 \tag{11}$$

where $Z = \partial T_p^{m+i-1}/\partial h_v^m$ and is called the sensitivity coefficient. It measures the rate of change in temperature due to change in the volumetric heat transfer coefficient. The idea here is to minimize equation (11) or, in other words, to make equation (11) approach zero by estimating a better value of h_v. Therefore, a better estimate of h_v can be expressed as [20]

$$h_{v,v}^m = h_{v,v-1}^m + \sum_{i=1}^{r} [T_e^{m+i-1} - T_{p,v-1}^{m+i-1}] Z_{v-1}^{m+i-1} / \sum_{i=1}^{r} [Z_{v-1}^{m+i-1}]^2. \tag{12}$$

Equation (10) is solved repeatedly until the change in h_v satisfies the criteria of minimum error, i.e.

$$\left| \frac{h_{v,v}^m - h_{v,v-1}^m}{h_{v,v}^m} \right| < \delta \tag{13}$$

where δ is taken to be 1×10^{-6}.

The steps to estimate the volumetric heat transfer coefficient h_v are:

(1) Estimate a value for h_v.

(2) Solve equations (6) and (7) for given boundary and initial conditions, equations (8), (9) and (5), as for experimentally obtained data.

(3) Since the analytical solution of the model equations is not possible, we need to determine Z numerically. Hence, add Δh_v to the estimated value of h_v and solve the energy equations (6) and (7) for the new heat transfer coefficient ($h_v + \Delta h_v$).

(4) Evaluate equation (11).

(5) Obtain a better estimate for h_v using equation (12).

(6) Repeat the procedure steps 2 through 5 by assuming the h_v value obtained from step 5 as an estimated value for step 2. Continue doing this until the desired criterion equation (13), is satisfied.

5. RESULTS AND DISCUSSION

5.1. *Data reduction and correlation*

The results of air temperature history close to the faces of the specimen were used to determine the volumetric heat transfer coefficient between the air stream and the solid matrix. The test conditions are summarized in Table 2. Based on the experimentally meas-

Table 2. Range of the experimental parameters

Operating conditions	Range
Density of matrix (kg m^{-3})	420–661
Average pore diameter (mm)	0.289–1.521
Porosity (%)	83–87
Thickness (mm)	12.0–14.0
Temperature of air (K)	335–351
Velocity (m s^{-1})	0.79–7.3

ured air temperatures, the average volumetric convection heat transfer coefficient is calculated by nonlinear matching of the experimentally determined temperature history with the one obtained numerically for a given Reynolds number and porous matrix properties. The temperature history is not smooth due to experimental errors; therefore, the data were first smoothed before using the data in the numerical model to determine the volumetric heat transfer coefficient.

The temperature distribution is corrected for error in the thermocouple measurements [15]. The maximum temperature measurement error due to conduction through the thermocouple leads is about 4.4% at times $t < 1.5$ s and much lower at later times. The corrected temperature is used in the theoretical model to determine the volumetric convective heat transfer coefficient by matching the experimental temperature vs time data with the predicted temperature vs time data using the nonlinear least-square fitting technique described.

The analysis yields the volumetric heat transfer coefficient h_v for each experiment and for each test specimen. Because of the importance of the solid matrix to fluid heat transfer coefficient in a porous ceramic, considerable effort has been devoted to evaluate this parameter. Because the surface area per unit volume of the porous ceramic specimen is unknown, the volumetric heat transfer coefficient is determined. The coefficient is averaged over the data time taking period. The time-averaged volumetric heat transfer coefficient over the operating period ranging from 15 to 40 s for the 0.94 mm mean pore diameter (designated by the manufacturer as 20 PPI, Pores Per Inch) alumina specimen for two flow rates are presented in Fig. 3. The variation of the coefficient with time is not significant. The data at the initial transient period (1–2 s) were ignored because of large error. Temperature correction was significant due to the transient caused by the insertion of the test specimen into the wind tunnel. The experimental uncertainty in determining the volumetric heat transfer coefficient is estimated to be 12.5% using an established technique [21]. The uncertainty analysis indicates that the thermophysical properties have an insignificant effect on the uncertainty of the volumetric heat transfer coefficient. The major uncertainty is attributable to the error in the temperature and velocity measurements. With the experimental arrangement and procedure used, the average experimental uncertainties in the Nusselt number and in the Reynolds number determination are 12.5% and 8.1%, respectively. Details of the uncertainty analysis and thermocouple error correction may be found elsewhere [15]. The effect of Nu_L and Nu_0 (equations (8) and (9)) on the uncertainty of the volumetric heat transfer was found to be insignificant (less than 0.5%).

The porous matrix consists of tortuous, irregularly shaped flow passages, and heat transfer takes place between the surface of the solid matrix and the fluid. For complex geometries, Kays and London [14] use the hydraulic diameter as a characteristic length to define the relevant dimensionless parameters for determining the heat exchanger performance. Unfortunately, for ceramic foams the hydraulic diameter cannot be readily determined. Foams can be visualized as a network of interconnected, nonuniform diameter tortuous passages through which flow takes place. The mean pore diameter (d) is very difficult to determine, but it appears to be a reasonable choice for the characteristic length in defining the Nusselt and Reynolds numbers.

The volumetric heat transfer coefficients are expressed in dimensionless form in terms of the Nusselt numbers. Figure 4 presents the Nusselt number vs Reynolds number dependence and shows a good fit. The least-square method was used to obtain a relationship between the Nusselt and Reynolds numbers. The following empirical correlation was obtained for the 0.94 mm mean pore diameter specimen,

$$Nu = 0.139\,Re^{0.92}, \quad 56 < Re < 370. \qquad (14)$$

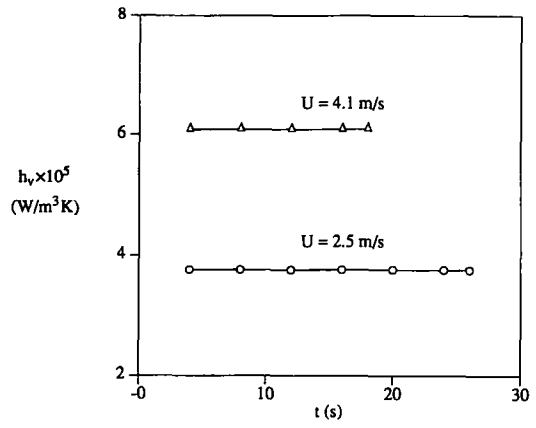

FIG. 3. Volumetric heat transfer coefficient vs time for 0.94 mm mean pore diameter alumina specimen.

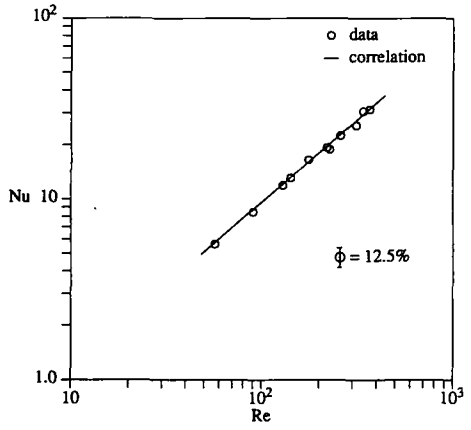

FIG. 4. Correlation of Nusselt vs Reynolds number for 0.94 mm mean pore diameter alumina specimen. Note the solid line is given by $Nu = 0.139Re^{0.92}$.

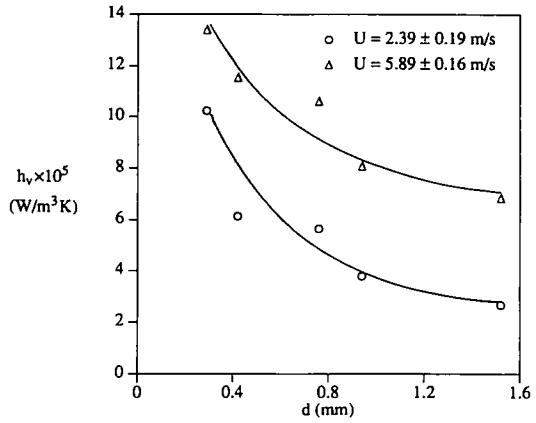

FIG. 5. Volumetric heat transfer coefficient vs mean pore diameter.

This relation cannot be compared with published correlations, since the flow passage is very complex and completely different than what has been reported in the literature. Also, it is noted that the exponent of the Reynolds number in this correlation (equation (14)) is different and higher than the one for either laminar flow (1/3) or turbulent flow (4/5) [22]. Convective heat transfer coefficients for screen matrices have been measured [14], and the data were correlated in terms of the Colburn j-factor, with the hydraulic diameter as the characteristic length in the Reynolds number. The Nusselt number in air using perfectly stacked screens can be represented as

$$Nu = C\,Re^m. \tag{15}$$

The constant C and the Reynolds number exponent m are 0.63 and 0.55, and 1.50 and 0.5 for porosities of 0.675 and 0.832, respectively.

5.2. *Heat transfer correlations*

Figure 5 presents the variation of the volumetric heat transfer coefficient vs the pore diameter for two velocities. The trends of the curves for the two velocities are almost identical and show that as the pore diameter increases the volumetric heat transfer coefficient decreases. Increasing the number of pores per mm of the test specimen yields different correlations. Table 3 lists the correlations obtained for porous alumina specimens having different mean pore diameters. The results indicate that the number of pores mm^{-1} affects the Nusselt number dependence on the Reynolds number. We attribute this to the fact that an increase in the pores mm^{-1} increases the surface area per unit volume and increases the convection heat transfer coefficient. It is, therefore, understandable why a decrease in the pore size should increase the volumetric convection heat transfer coefficient ($h_v = a_v h$).

Table 3. Nusselt vs Reynolds numbers correlation for (92% Al_2O_3) ceramic foam specimen

Average pore diameter (mm)	Velocity ($m\,s^{-1}$)	d/L	Reynolds number	Correlation
1.52	1.24–6.75	0.117	103–563	$Nu = 0.146\,Re^{0.96}$
0.94	1.00–7.15	0.079	56–370	$Nu = 0.139\,Re^{0.92}$
0.76	1.20–6.37	0.067	50–266	$Nu = 0.456\,Re^{0.70}$
0.42	1.16–6.48	0.035	26–150	$Nu = 0.485\,Re^{0.55}$
0.29	1.56–5.72	0.023	24–91	$Nu = 0.638\,Re^{0.42}$

The correlations for the five alumina samples have been plotted in Fig. 6. The figure shows that the data are well correlated for each sample. The experimental data points fit the correlation line for 1.52, 0.94 and 0.76 mm mean pore diameters well, while for 0.42 and 0.29 mm pore diameters the data depart from the curve fit. For the small pore diameters dust and other particles in the laboratory air may have affected the mean pore diameter for these specimens during the experiment and caused scatter of the data. The pore diameter changed during the course of the experiment due to the accumulation of very fine particulate matter on the porous surface. Visual and microscopic examinations revealed this change very clearly, but no quantitative measurements were made. This conclusion was reached after each experiment was repeated at least three times. As the number of pores per mm decreases, the dependence of the Nusselt number on the Reynolds number also changes. For $Re > 100$, the effect of pore size is large, particularly for 1.52 mm pore diameter specimen. For each test specimen the maximum Reynolds number range covered was within the design capability of the test apparatus. As shown, the data at high Reynolds numbers are consistent; however, at low flow rates the data indicate a continuous decrease in the Nusselt number with decreasing Reynolds number [22]. This anomalous decrease in the Nusselt number at low Reynolds numbers has been the subject of long dispute. There are two opposing views: one supports the unlimited decrease in the Nusselt number based on experimental observations, whereas the others argue that a limiting Nusselt number should exist at zero

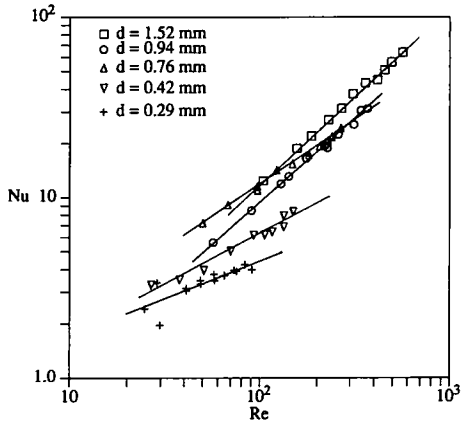

FIG. 6. Correlation of Nusselt vs Reynolds number for five alumina samples.

flow rate. Some investigators have shown from frequency response measurements that the limiting Nusselt number is about 10 [23]. Huber and Jones [9] have pointed out that the small Nusselt numbers at low Reynolds numbers may occur because only part of the particle surface is accessible to the fluid. As a result of this particle–fluid interaction, they proposed an empirical equation based on their experimental data. The experimental results obtained in the present study support the first view. However, further studies at low Reynolds numbers are required to clarify this point, since the minimum Reynolds number obtained is not very low or close to zero. The results show that as pore diameter increases the exponent of the Reynolds number also increases.

The empirical correlation found to be obtained using a least-square fit is

$$Nu = 0.819[1-7.33(d/L)]\,Re^{0.36[1+15.5(d/L)]}. \quad (16)$$

It is based on the experimental data for the following range of parameters: $0.005 < d/L < 0.136$ and $5.1 < Re < 564$. The correlation fits the data best for low number of pores cm^{-1} with a maximum deviation being less than 2%, but for larger number of pores mm^{-1} (number of pores $cm^{-1} = 26$) the maximum deviation is about 27.1%. The discrepancy between the correlation and data for large number of pores cm^{-1} (26) is due to the accumulation of particulate matter on the porous surface from the laboratory air during the experiments.

The cordierite specimen was not included in the correlating equation (16), because the results obtained with the specimen differed significantly from the alumina specimen. Equation (16) is restricted to the range of Reynolds numbers investigated experimentally. Only rather limited experimental data for the cordierite specimen had been obtained, and the effect of d/L had not been investigated. The change in d/L is primarily due to the change in the pore diameter (d), because the thickness (L) of the specimen used was approximately the same (see Table 2).

A comparison of the Nusselt number obtained from equation (16) with the Nusselt number calculated from correlations for packed beds [24] and sintered metals [25, 26] is shown in Fig. 7. The figure reveals that Nusselt numbers for ceramic foams are higher than those of packed beds and sintered metals. We attribute this to the fact that the porosity of ceramic foam (0.83 to 0.87) is much larger than the porosity of the packed beds of sintered metals (0.35 to 0.55). Also, the structure of the materials is different, which has a large influence on the convective heat transfer, because the material affects the shape and the flow passage diameter as well as the surface area per unit volume.

5.3. *Cordierite test specimen*

A test specimen made from cordierite was used for a range of velocities. For a mean pore diameter of

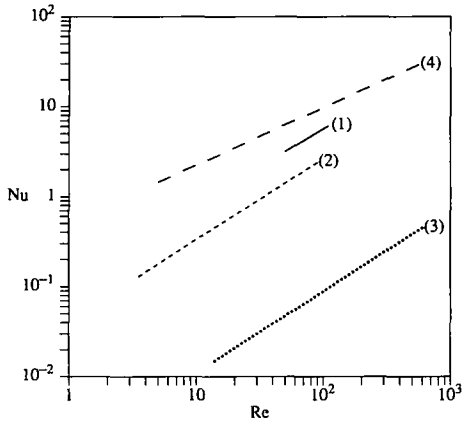

FIG. 7. Comparison of Nusselt number of equation (16) with correlation of the packed bed and sintered metals: (1) packed bed, $Nu = 0.124\ Re^{0.83}$, $50 < Re < 100$ [24]; (2) sintered metal, $Nu = 0.042\ Re^{0.91}$, $3.5 < Re < 90$ [25]; (3) sintered metal, $Nu = 0.0014\ Re^{0.91}$, $3.5 < Re < 600$ [26]; (4) ceramic foam, $Nu = 0.819[1-7.33(d/L)]\ Re^{0.36[1+15.5(d/L)]}$, $5.1 < Re < 563$ (present work).

1.27 mm (which corresponds to 20 PPI) the Nusselt vs Reynolds correlation obtained is

$$Nu = 2.43\,Re^{0.42}, \quad 65 < Re < 457. \quad (17)$$

A comparison of the cordierite and alumina specimen correlations for the same number of pores per unit of thickness (20 PPI) is given in Fig. 8. There is considerable difference between the results for the two samples, because the shape of the flow passage, mean pore diameter, and porosity are different. The mean pore diameter for the cordierite test specimen was calculated from the number of pores per inch provided by the manufacturer (Bridgestone Corporation). The mean pore diameters differ by about 25%. For the same test specimen, Ishibashi [27] has calculated the mean pore diameter to be 0.635 mm. The measured volumetric convective heat transfer coefficients based on this mean pore diameter are also presented in Fig. 8 and can be correlated by the equation

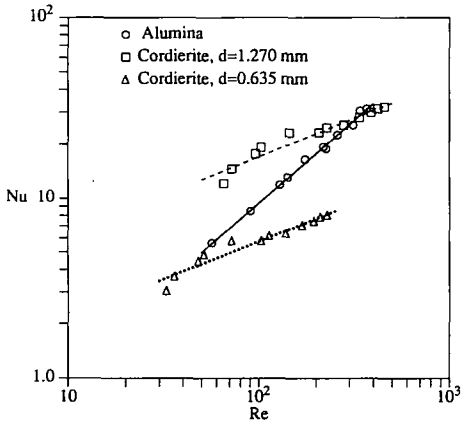

FIG. 8. Correlation of Nusselt vs Reynolds number for 8 pores per cm (20 PPI) alumina and cordierite specimen.

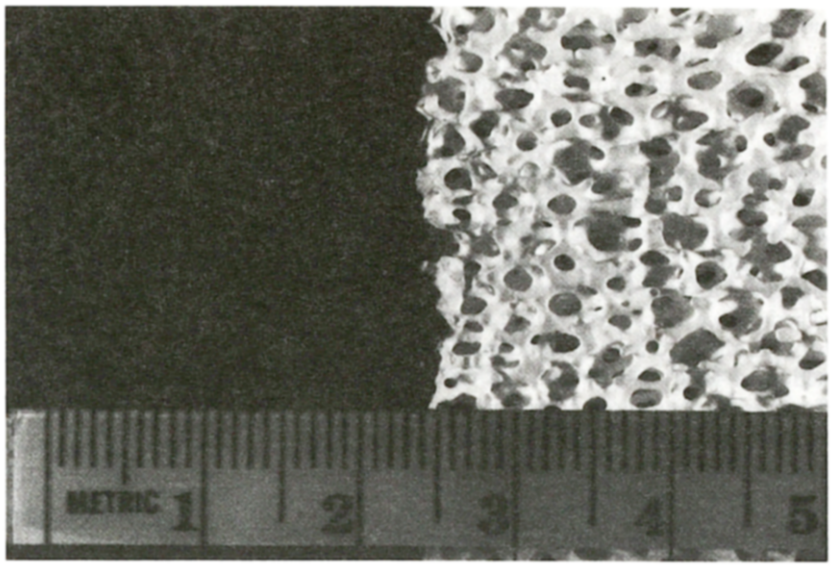

FIG. 9. Photograph of the 8 pores per cm (20 PPI) alumina test specimen manufactured by Bridgestone Corporation (left), and Hi-Tech Ceramics, Inc. (right)

$$Nu = 0.824\, Re^{0.42}, \quad 32 < Re < 229. \qquad (18)$$

Figure 8 reveals that at $Re = 345$ the two specimens (alumina and cordierite) have the same Nusselt number. The results presented in this figure clearly demonstrate that the choice of a characteristic length in the Nusselt and Reynolds numbers is very important. The results also reveal that the mean pore diameter does not affect the Reynolds number exponent, but it lowers the Nusselt number significantly. This is to be expected from the definition of Nu.

The largest difference between the two test specimens is attributed to the mean pore diameters and the shape of the tortuous flow passages. Figure 9 shows a photograph of the 8 pores per cm (20 PPI) specimen of alumina and cordierite. It is evident from the photograph that there is a difference in the flow passages for the two test specimens. Some of the pores near the face of the cordierite ceramic foam specimen are completely blocked, whereas those of the alumina are open. The blockage of flow in some cells and the different shape and structure of the solid matrix are believed to be the main reasons for the differences in the volumetric heat transfer coefficient. The finding suggests that more detailed features of the geometry of the porous structure (i.e. flow passage) will have to be considered in obtaining more general convective heat transfer correlations.

6. CONCLUSIONS

Heat transfer by forced convection of air in porous ceramic foams was investigated experimentally. The governing conservation equations of energy for both the gas and the solid and the corresponding boundary conditions were solved using a finite-difference procedure. A nonlinear least-square fitting of temperature in conjunction with an inverse method was applied to determine the volumetric heat transfer coefficient between air and ceramic foams. Experiments were performed on foams having different mean pore diameters, and the heat transfer coefficient correlations were obtained from each pore diameter ceramic foam tested.

The major conclusions based on our numerical and experimental studies are as follows:

- The downstream temperature distribution in the gas was measured. A comparison between predicted and measured temperatures yielded the volumetric heat transfer coefficients.
- The volumetric heat transfer coefficient was determined, and it showed strong dependence on the mean pore diameter. As the pore diameter increased the volumetric heat transfer coefficient decreased. The average heat transfer coefficient was nearly constant over the time period during which data were taken.
- A Nusselt vs Reynolds number heat transfer correlations were obtained for each ceramic foam tested. It was found that the exponent of the Reynolds number decreased with the decrease in the pore diameter.
- For different pore sizes a correlation was obtained for the entire range of Reynolds numbers and L/d, although the thickness L of the ceramic foam was changed only slightly.
- Alumina and cordierite ceramic foams were used, and heat transfer results were compared. The Nusselt numbers obtained for the cordierite specimen are higher than those for the alumina specimen for low Reynolds number, but the Nusselt numbers for both test specimens approached each other and became identical for $Re = 345$. The Reynolds number exponent of the alumina specimen was found to be larger than that for cordierite.

• The difference between the volumetric heat transfer coefficients determined in this work for ceramic foams and those for packed beds and sintered metals reported in the literature is attributed primarily to three reasons. First, the flow passages in ceramic foams are tortuous and differ significantly from those in packed beds and sintered metals. Second, the surface areas per unit volume differ greatly for the different geometrical structures. Third, the porosities of ceramic foams are about a factor of two greater than those for packed beds. Since the convective heat transfer coefficient between the fluid and the solid matrix is a strong function of local velocity and the flow passage, the differences in heat transfer characteristics between ceramic foams and packed beds or sintered metals are not unexpected.

The findings of this study have clearly demonstrated that the problem of convective heat transfer between a fluid and a ceramic foam is complex and needs further research attention to identify fundamental phenomena and obtain predictive heat transfer equations for these materials. Experimental studies are needed to measure the surface area per unit volume, passage geometry and to determine the reasons for the differences in the heat transfer characteristics of ceramic foams of the same composition but manufactured in a different manner. Additional studies are needed to clarify the dependence of the volumetric heat transfer coefficient on the sample thickness to the mean pore diameter ratio (L/d). Heat transfer coefficients at low velocities (small Re) need to be measured to establish asymptotic behavior of Nu vs Re. Finally, an appropriate characteristic length for defining the Nusselt and Reynolds numbers for foam-like materials needs to be determined.

REFERENCES

1. R. Viskanta, Enhancement of heat transfer in industrial combustion systems: problems and future challenges, *Proceedings of the Third ASME/JSME Joint Thermal Engineering Conference* (Edited by J. R. Lloyd and Y. Kurosaki), Vol. 5, pp. 163–173. ASME/JSME, New York (1991).
2. F. Anderson, Heat transport model for fibre burners, *Prog. Energy Combust. Sci.* **18,** 1–12 (1991).
3. T.-Y. Xiong, D. K. Fleming and S. A. Weil, Hazardous material destruction in a self-regulating combustor-regenerator, *Emerging Technologies in Hazardous Waste Management II* (Edited by D. W. Tedder and F. G. Pohland), pp. 12–28. American Chemical Society, Washington, D.C. (1991).
4. V. A. Maiorov, L. L. Vasil'ev and V. M. Polyaev, Porous heat exchangers—classification, construction, application, *J. Engng Phys.* **47,** 1110–1123 (1984).
5. V. M. Eroshenko and L. A. Yaskin, Heat transfer in forced convection of fluid in porous sintered metals, *J. Engng Phys.* **30,** 1–7 (1976).
6. A. G. Dixon and D. L. Cresswell, Theoretical prediction of effective heat transfer parameters in packed beds, *Am. Inst. Chem. Engng* **25,** 663–676 (1979).
7. A. R. Balakrishnan and D. C. T. Pei, Heat transfer in gas–solid packed beds system 3. Overall heat transfer rates in adiabatic beds, *Ind. Engng Chem. Process Des. Dev.* **18,** 47–50 (1979).
8. O. M. Alifanov, A. P. Tryanin and A. L. Lozhkin, Experimental investigation of the method of determining the internal heat-transfer coefficient in a porous body from the solution of the inverse problem, *J. Engng Phys.* **52,** 340–346 (1987).
9. M. L. Huber and M. C. Jones, A frequency response study of packed bed heat transfer at elevated temperatures, *Int. J. Heat Mass Transfer* **31,** 843–853 (1988).
10. M. Golombok, H. Tariwala and L. C. Shirvill, Gas–solid heat exchange in a fibrous metallic material measured by a heat regenerator technique, *Int. J. Heat Mass Transfer* **33,** 243–252 (1990).
11. T. E. Schumann, Heat transfer of a liquid flowing through a porous prism, *J. Franklin Inst.* **208,** 405–416 (1929).
12. C. C. Furnas, Heat transfer from a gas stream to a bed of broken solid, Bull. U.S. Bureau of Mines, No. 261 (1932).
13. B. I. Kitaev, Yu. G. Yaroshenko and V. D. Suchkov, *Heat Exchange in Shaft Furnaces.* Pergamon Press Ltd, London (1967).
14. W. M. Kays and A. L. London, *Compact Heat Exchangers* (2nd Edn). McGraw-Hill, New York (1964).
15. L. B. Younis, Experimental determination of the volumetric heat transfer coefficient between a stream of air and a ceramic foam, Thesis, Purdue University, W. Lafayette, IN (1991).
16. P. F. Pucci, C. P. Howard and C. H. Piersall, Jr., The single-blow transient testing technique for compact heat exchanger surfaces, *J. Engng Power* **89,** 29–40 (1967).
17. D. Vortmeyer, Axial heat dispersion in packed beds, *Chem. Engng Sci.* **30,** 999–1001 (1975).
18. A. P. Tryanin, Determination of heat transfer coefficients at the inlet into a porous body and inside it by solving the inverse problem, *J. Engng Phys.* **42,** 346–351 (1987).
19. S. V. Patankar, *Numerical Heat Transfer and Fluid Flow.* Hemisphere, New York (1980).
20. J. V. Beck and B. Blackwell, *Inverse Heat Conduction.* Wiley, New York (1985).
21. R. J. Moffat, Describing the uncertainties in experimental results, *Exp. Thermal Fluid Sci.* **1,** 3–17 (1988).
22. N. Wakao and S. Kaguei, *Heat Transfer in Packed Beds.* Gordon & Breach Science Publishers, New York (1982).
23. D. J. Gunn and J. F. C. De Souza, Heat transfer and axial dispersion in packed beds, *Chem. Engng Sci.* **29,** 1363–1371 (1974).
24. A. F. Ckechetkin, *High Temperature Heat Carriers.* Pergamon Press Ltd, Oxford (1963).
25. V. N. Karchenko (1968) Cited by V. M. Eroshenko and L. A. Yaskin, Heat transfer in forced convection of fluid in porous sintered metals, *J. Engng Phys.* **30,** 1–8 (1976).
26. R. Bernicker, An investigation of porous wall cooling, ASME Paper 60-WA-233, ASME, New York (1960).
27. M. Ishibashi, Personal communication, Bridgestone Corporation, April 13, 1992.